ChemComm

Accepted Manuscript

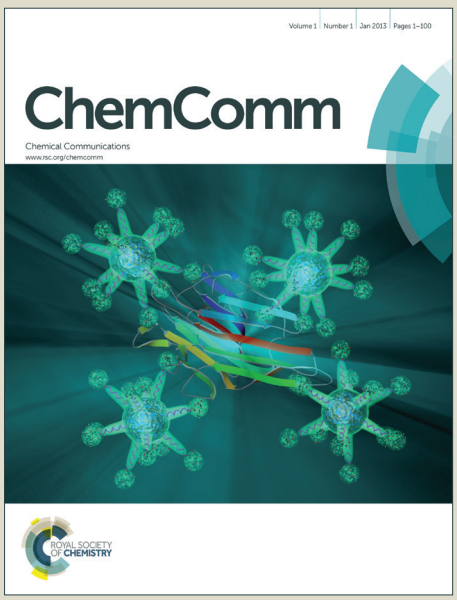

ROYAL SOCIETY OF CHEMISTRY

www.rsc.org/chemcomm

RSCPublishing

Crystallization of hollow mesoporous silica nanoparticles

Cite this: DOI: 10.1039/x0xx00000x

Glenna L. Drisko,[a,b,À] Adrian Carretero-Genevrier,[a,c,À*] Alexandre Perrot,[a] Martí Gich,[d] Jaume Gàzquez,[d] Juan Rodriguez-Carvajal,[e] Luc Favre,[f] David Grosso,[a,g] Cédric Boissière,[a,h] Clément Sanchez[a,g,h,*]

Received 00th January 2012,
Accepted 00th January 2012

DOI: 10.1039/x0xx00000x

www.rsc.org/

Complex 3D macrostructured nanoparticles are transformed from amorphous silica into pure polycrystalline Ŭ-quartz using catalytic quantities of alkaline earths as devitrificants. Walls as thin as 10 nm could be crystallized without losing the architecture of the particles. The roles of cation size and the mol% of incorporated devitrificant on crystallization behavior are studied, with Mg^{2+}, Ca^{2+}, Sr^{2+} and Ba^{2+} all producing pure Ŭ-quartz under certain conditions.

Despite the fact that Si compounds are major components of the lithosphere, very few examples of structured SiO_2 can be found in the living world, the major exception being diatoms.[1] The construction of amorphous structured SiO_2 through solution chemistry has been mastered in synthetic materials, however the extension to crystallized SiO_2 has faltered. In spite of a variety of potential applications, the delayed development of crystallized nanostructured silica is largely due to the difficulty in devitrifying and preserving small features at ambient pressure and the temperatures achievable in standard laboratory furnaces. In SiO_2 crystallization the nucleation to growth ratio is typically very low,[2] leading to inhomogeneous nucleation, growth of very large crystals and loss of nanoscopic morphologies. Also due to the slight differences in the energy between amorphous, and crystalline silica polymorphs, it is often difficult to obtain a pure and highly crystalline phase.[3]

To simultaneously crystallize and retain nano-sized SiO_2 particles, hydrothermal synthesis has been employed using amorphous silica.[2,4,5] By controlling salt concentration, pressure and treatment time, both crystalline phase and particle size could be influenced.[4] The size of the initial silica particles has bearing on the final crystalline particle size,[5] though it is not certain that this size correlation is due to the seeds themselves being crystallized without dissolution-recrystallization as the solution incorporates NaOH that dissolves silica and NaCl that tends to induce precipitation and is known to promote devitrification. Crystalline SiO_2 nanoparticles have also been produced by adding Ti^{4+} and Ca^{2+} dopants to the silica matrix and then calcining at ambient pressure and 1000 °C.[6] The onset of crystallization is dependent on both the temperature and the mol% of dopant in the silica.[7] By incorporating Sr^{2+} or Ba^{2+} salts into mesoporous thin films, pure Ŭ-quartz could be grown under relatively mild conditions with an epitaxial relationship to a Si-substrate.[8-10] Here we present the first preparation of crystalline SiO_2 nanoparticles with well-defined, complex morphologies. The particles contain an inner cavity, which is fully preserved upon crystallization. The synthetic conditions have been varied so that Ŭ-quartz can be produced without contamination from cristobalite or other crystalline SiO_2 phases. The effect of devitrificant nature on crystallization has been examined to deeply understand the crystallization process. The crystallization behavior deviates from what has been observed in the crystallization of nanostructured thin films.[8-10] Structured monocrystalline quartz nanoparticles can be incorporated into optical devices due to their difference in refractive index with respect to amorphous silica and transparency in the UV-visible to near IR range of the spectrum. Alternatively, quartz particles can be used as abrasives,[11] as highly effective supports for photocatalysts[12] and nanolubricants.[13]

This work develops a novel method to easily prepare hollow quartz (low quartz) nanoparticles grown by sol-gel and template chemistry. Briefly, crystalline silica nanoparticles with an intact nanocavity were obtained from an amorphous mesoporous silica shell (Figure 1). To prepare the amorphous nanoparticles, polystyrene latexes were coated with mesoporous silica, derived from the hydrolysis and condensation of TEOS in the presence of CTAB.[14] Centrifugation of the hybrid particles generated a monolith of closely packed spheres. This monolith was calcined to remove the organic templates and then infiltrated with a solution containing an alkaline earth salt, which catalyzed the crystallization of silica. The meso- and macroporosity acted as reservoirs for the salt solution,

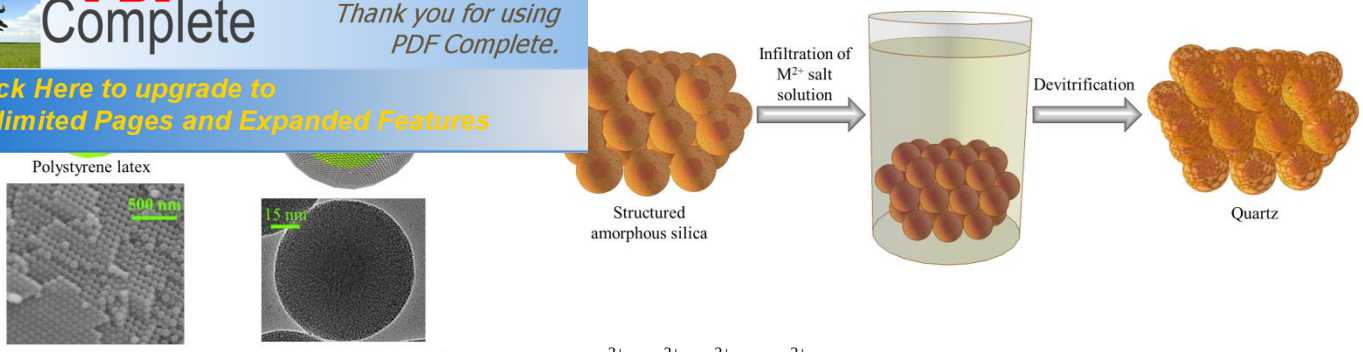

Fig. 1 Hollow mesoporous silica shells are infiltration with Mg^{2+}, Ca^{2+}, Sr^{2+} or Ba^{2+} and then crystallization between 800-1000 °C.

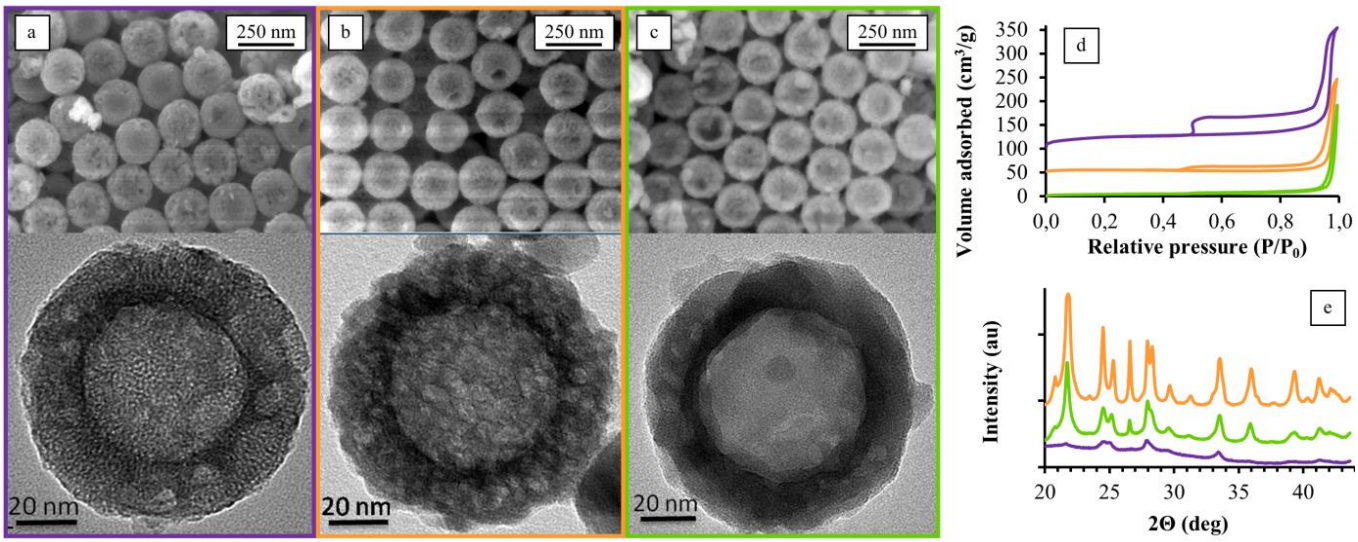

Fig. 2 SEM and TEM micrographs of particles calcined for 5 h under air at (a) 800, (b) 900 and (c) 1000 °C. (d) Nitrogen sorption isotherms of these particles calcined at 800 (purple line, shifted up the y-axis +100), 900 (orange line, shifted up the y-axis +50) and 1000 °C (green line). (e) X-ray diffraction patterns of these same particles, represented by the same color scheme.

allowing the homogeneous devitrification of the silica shell, similarly to the strategy previously reported for thin films.[8-10] Without widespread salt partitioning in the amorphous network, it is unlikely that the structure could have been maintained and fully crystallized.

The role of the crystallization temperature was studied after infiltration of the particles with a 1 M solution of $Sr(NO_3)_2$. Previously cristobalite has been crystallized at low temperature (750 °C) by applying low pressure (4 Torr).[15] Here, ambient pressure crystallization began at 800 ºC and was fully completed by 900 ºC (Figure 2 and S4). Despite continued crystallite growth with increasing temperatures up to 1000 ºC, the integrity of the nanocavity was preserved. The key point in this process is the incorporation of an alkaline earth cation, which creates non-bridging oxygens, thus enabling the reorganization of the SiO_2 network. Alkali ions also give rise to non-bridging oxygens (NBO) but their mobility in glass is much higher than that of alkaline earth ions which are indeed introduced in soda lime glass to increase its chemical resistance.[16] The alkaline earths prove to be gentle devitrificants, allowing confined crystallization to occur without large scale melting and loss of morphology, which was not the case for Li^+. Lithium is known to be an excellent melting agent and when infiltrated into the amorphous mesoporous silica shells, highly crystalline samples were obtained at temperatures as low as 650 ºC with a total loss of structure (Figure S2). Conversely, silica crystallization was not observed in the absence of an alkaline earth metal at a temperature of 900 °C which means that the presence of the melting agent induces nanoparticle crystallization (Figure S3).

The 3 nm sized mesopores generated from CTAB templating collapsed upon crystallization, observed via decreasing pore volume, as detected by N_2-sorption measurements (Figure 2d). The disappearance in mesoporosity is due to diffusive sintering.[10] The surface area correspondingly decreased from 1281 $m^2 g^{-1}$ (800 °C) to 17 $m^2 g^{-1}$ (900 °C) to 16 $m^2 g^{-1}$ (1000 °C). Thus it seems likely that the majority of these crystallized nanoparticles possess intact shells.

The quartz crystallite size was determined for polycrystralline particles infiltrated with Sr^{2+} using the Voigt function model for the intrinsic and the instrumental profile of X-ray patterns as implemented in the Fullprof program.[17] The analysis was performed simultaneously with the structural Rietveld refinement (Figure S4). The degree of crystallinity and the crystallite size grew with increasing calcination temperature (Figure 2a-c, e and Figure S4). We observed that silica nanoparticles calcined at 800 °C in the presence of Sr^{2+} are composed of quartz crystallites with an average grain size of 5.3 nm. Quartz crystallite size increased with calcination temperature to 35.2 nm at 900° C and then further to 43.8 nm at 1000 °C. The distances between atomic planes oriented at 60° from each other observed in the HRTEM image are 4.26 Å and 4.26 Å, corresponding to the d-spacings of the (100) and (010) planes viewed along the [001] zone axis of a single quartz crystallite with hexagonal settings (Figure 3b). The diffraction pattern generated by the Fast Fourier Transform (FFT) confirms that most of the particle

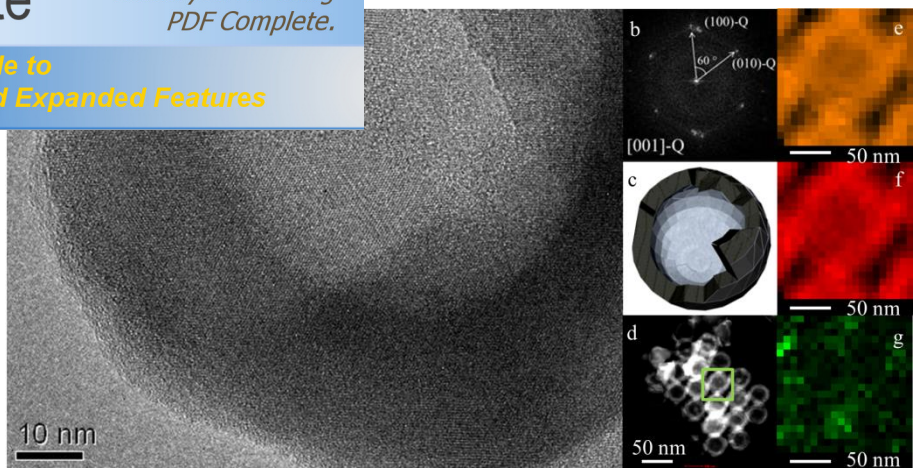

Figure 3. (a) HRTEM image and (b) corresponding diffraction pattern generated by the FFT of image (a) for a particle calcined at 900 °C for 5 h under air. (c) Depiction of a broken particle, like that displayed in (a). (d) STEM and elemental mapping of KŬ emissions of (e) Si, (f) O and (g) Sr for particles calcined at 1000 °C for 5 h under air.

is crystallized into the trigonal Ŭ-quartz polymorph. Elemental mapping via high-angular annular dark field image (HAADF) scanning transmission electron microscopy (STEM) (Figure 3d) was used to give information about the distribution of Sr^{2+} within particles infiltrated with $Sr(NO_3)_2$ and calcined at 1000 ºC. The brighter regions correspond to Sr, which is principally located in exterior regions of the silica nanoparticles. A detailed distribution of elements through a silica nanoparticle was performed using STEM in combination with electron-energy-loss spectroscopy (EELS). Figure 3e, f, and g display the elemental maps corresponding to the O, Si and Sr K edges, showing the elemental distribution across a single nanoparticle. The elemental mapping shows that strontium is distributed throughout the spheres with elevated concentration at the contact points with other particles (Figure 3g). Previously it has been shown in the crystallization of thin films that Sr^{2+} migrates to the quartz crystal boundaries to minimize the surface energy of the $SrCO_3$ particles which form after the crystallization treatment.[9] An analogous behavior seems to be observed in these particles.

A series of alkaline earth metals (Mg^{2+}, Ca^{2+}, Sr^{2+} and Ba^{2+}) were tested for their ability to crystallize amorphous silica and the diffraction patterns recorded for these materials are presented in Figure 4. All of the studied cations were able to crystallize silica to produce Ŭ-quartz without parasitic crystalline phases, while preserving the morphology of the nanocavity. However for Ca^{2+} and Sr^{2+}, a residual amorphous phase remained after the applied crystallization treatments. Cristobalite was not observed in these studies. A cation-dependent selectivity has previously been reported in hot-pressed gels, where Na^{+} favors the formation of cristobalite and Li^{+} that of Ŭ-quartz.[18] Upon increasing the concentration of devitrificant in the silica particles, a silicate phase appeared after thermal treatment (Figure S5). In the case of strontium, the new phase is unknown and additional phases appear upon further increasing the strontium quantity in the silica matrix (Figure S4 and S6). Currently investigations are underway to identify these unknown phases.

As the size of the cation increased, the minimum salt concentration needed to induce crystallization decreased (Figure 4). In silicate glasses, as alkaline earth cations increase in size, the coordination numbers and NBO/Si ratios increase due to large ionsô lower field strength, Z/r^2 where Z is the valence and r the ionic radius.[19] The silica gels studied in this work are likely to display a similar behavior and thus a lower concentration of the larger alkaline earth cations is enough to reach the critical concentration of NBOs and trigger devitrification.

To study the crystallization of thinner walls, an aerosol containing latexes, TEOS and $BaCl_2$ was prepared by spray-drying (Figure S7). The evaporation of the solvent led to the condensation

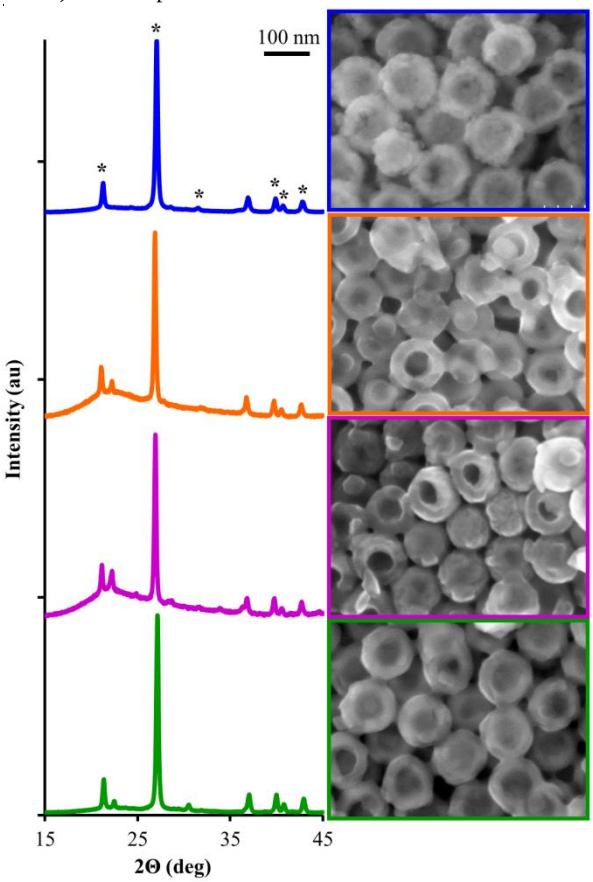

Fig. 4 WAXS pattern of particles treated at 1000 °C for 5 h in air with molar compositions 0.1 Mg^{2+}:1 Si (blue), 0.025 Ca^{2+}:1 Si (orange); 0.02 Sr^{2+}:1 Si (purple); and 0.01 Ba^{2+}:1 Si (green). The peaks were indexed according to the ICDD, card no. 09-8780 corresponding to Ŭ-quartz (*). The minimum salt concentration to generate Ŭ-quartz was employed. All images are the same scale.

rk. Heat
ue to the
thermal
re could
extended
thermal treatment times, diffusive sintering increased wall thickness.

The crystallization behavior in these nanoparticles differs dramatically from that seen in thin films, where the epitaxial relationship with the crystalline silicon substrate directed the crystallization behavior. In films, an excess of devitrificant prevented crystallization.[10] Here an excess led to the formation of an alkaline earth-silicate phase. Also, the optimal amount of strontium differed between the particles and films. Whereas in the case of films the quartz crystallization was maximized at a Sr:Si molar ratio of 0.06, this same concentration produced an unknown silicate phase in the particles. Conversely, in the particles at a Sr:Si molar ratio of 0.02 non-contaminated Ŭ-quartz was obtained, whereas in films this ratio did not crystallize the silica matrix. These observed differences and the polycrystallinity of the nanoparticles result from the absence of direct contact with a crystalline substrate.

Conclusions

Alkaline earth salts provided a new route to the preparation of pure polycrystalline Ŭ-quartz nanoparticles with complex morphologies. These salts can be included into the amorphous matrix through either post-synthetic infiltration into the mesoporous silica shells, or in a one-pot synthesis via aerosol. Crystallization at ambient pressure and 800 ºC is possible thanks to the devitrificant inclusion within the silica network.

A series of alkaline earth metals show that as cation size increases, less devitrificant is needed to induce the crystallization. Irrespective of the cation used in this study, feature sizes of 80 nm were well conserved and wall thicknesses as low as 10 nm were faithfully preserved.

To date material scientists have mastered control over amorphous silica morphologies, but this is the first report where these free floating structures can be crystallized without deleterious effects on the morphology. Other silica structures can be similarly crystallized by adjusting the cation to silica surface area. The hollow quartz nanoparticles reported in this work could find applications in the field of optics thanks to the hardness, low solubility, piezoelectric response, high refractive index and broad range transparency of this silica polymorph.

Acknowledgements
ACG and GLD acknowledge the Collège de France foundation and Solvay for financial support and IMPC for use FEG-SEM facilities. We thank David Montero and Mohamed Selmane for technical support. Cellule Energie INSIS-CNRS awarded ACG with project PEPS (1D-RENOX). The Spanish Ministerio de Economía y Competitividad and the European Comission respectively awarded RyC-2012-11709 grant to JG and PCIG09-GA-2011-294168 to MG. Some microscopy was conducted in the Laboratorio de Microscopias Avanzadas at Instituto de Nanociencia de Aragon-Universidad de Zaragoza. LMA-INA provided access to their instruments and expertise.

Notes and references

[a] *Collège de France, UMR 7574, Chimie de la Matière Condensée de Paris, F-75005, France. E-mail: clement.sanchez@college-de-france.fr*
[b] *Laboratoire de Chimie de Coordination, CNRS UPR8241, 205, route de Narbonne, 31077 Toulouse, France.*
[c] *Institut des Nanotechnologies de Lyon (INL) CNRS 69134 Ecully, France. E-mail: adrien.carretero-genevrier@ec-lyon.fr*
[d] *Institut de Ciència de Materials de Barcelona, Bellaterra 08193, Spain*
[e] *Institut Laue-Langevin, Diffraction Group, F-38042 Grenoble, France*
[f] *IM2NP, Faculté des Sciences et Techniques, Campus de Saint Jérôme - Case 142, Avenue Escadrille Normandie Niemen, 13397 Marseille* [g] *Sorbonne Universités UPMC Univ Paris 06, UMR 7574, Chimie de la Matière Condensée de Paris, F-75005, Paris, France.*
[h] *CNRS, UMR 7574, Chimie de la Matière Condensée de Paris, F-75005, Paris, France.*
À These authors contributed equally to this work.
Electronic Supplementary Information (ESI) available: experimental protocols, SEM and TEM images of nanoparticles and aerosols, WAXS and SAED analysis of crystalline nanoparticles, Rietveld refinement and pattern matching analyses and. See DOI: 10.1039/c000000x/

1 N. Nassif, J. Livage, *Chem. Soc. Rev.* 2011, **40**, 849.
2 J. F Bertone, J. Cizeron, R. K. Wahi, J. K. Bosworth, V. L. Colvin, *Nano Lett.* 2003, **3**, 655.
3 A. Navrotsky,*"Thermochemistry of Silica" in Reviews in Mineralogy*; P. J. Heaney, C. T. Perwitt, G. V. Gibbs, Eds.; Mineralogical Society of America: 1994; Vol. 29 p309-329.
4 K. Yanagisawa, Y. Zhu, A. Onda, K. Kajiyoshi, *J. Mater. Sci.* 2004, **39**, 2931.
5 X. Jiang, Y. B. Jiang, C. J. Brinker, *Chem. Commun.* 2011, **47**, 7524.
6 M. Okabayashi, K. Miyazaki, T. Kono, M. Tanaka, Y. Toda, *Chem. Lett.* 2005, **34**, 58.
7 Z. Congshan, J. Phalippou, J. Zarzycki, *J. Non-Crystalline Solids* 1986, **82**, 321.
8 A. Carretero-Genevrier, M. Gich, L. Picas, J. Gàzquez, G. L. Drisko, C. Boissiere, D. Grosso, J. Rodriguez-Carvajal, C. Sanchez, *Science* 2013, **340**, 827.
9 G. L. Drisko, A. Carretero-Genevrier, M. Gich, J. Gàzquez, D. Ferrah, D. Grosso, C. Boissiere, J. Rodriguez-Carvajal, C. Sanchez, *Adv. Funct. Mater.* 2014, **24**, 5494.
10 A. Carretero-Genevrier, G. L. Drisko, D. Grosso, C. Boissiere, C. Sanchez, *Nanoscale* 2014, **6**, 14025.
11 M. Mosleh, K. A. Shirvani, *Wear* 2013, **301**, 137.
12 I. N. Martyanov, K. J. Klabunde, *J. Catalysis* 2004, **225**, 408.
13 S. Y. Sia, E. Z. Bassyony, A. A. D. Sarhan, *Int. J. Adv. Manuf. Technol.* 2014, **71**, 1277.
14 H. Blas, M. Save, P. Pasetto, C. Boissière, C. Sanchez, B. Charleux, *Langmuir* 2008, **24**, 13132.
15 X. Jiang, L. Bao, Y. S. Cheng, D. R. Dunphy, X. Li, C. J. Brinker, *Chem. Commun.* 2012, **48**, 1293.
16 E. Le Bourhis, Glass: Mechanics and Technology, Wiley-VCH Verlag: 2007, p57-58.
17 Rodriguez-Carvajal, J. In *"FULLPROF: A program for Rietveld refinement and pattern matching analyses."* International Union of Crystallography: Chester, England: Toulouse, France, 1990, p 127.
18 J. Phalippou, M. Prassas, J. Zarzycki, *J. Non-Crystalline Solids* 1982, **48**, 17.
19 C.-C. Lin, S.-F. Chen, L. Liu, C.-C. Li *Mater. Chem. Phys.* 2010, **123**, 569.